Nuclear Engineering and Design, 333 (2018) 181-195, https://doi.org/10.1016/j.nucengdes.2018.04.015

Pre-test analysis of accidental transients for ALFRED SGBT mock-up characterization

Vincenzo NARCISI[a], Fabio GIANNETTI[a], Alessandro DEL NEVO[b], Mariano TARANTINO[b], Gianfranco CARUSO[a]

Corresponding author: Vincenzo Narcisi (vincenzo.narcisi@uniroma1.it)

a) DIAEE - Nuclear Section, “Sapienza” University of Rome, Corso Vittorio Emanuele II, 244, 00186, Roma, Italy

b) Italian National Agency for New Technologies, Energy and Sustainable Economic Development, C.R. ENEA Brasimone, Italy

Abstract

In the framework of the Horizon 2020 SESAME project (thermal hydraulics Simulations and Experiments for the Safety Assessment of MEtal cooled reactors), the CIRCE pool facility has been refurbished by ENEA to host HERO test section (Heavy liquid mEtal pRessurized water cOoled tubes) with the aim to test an innovative concept of the steam generator bayonet tubes proposed for ALFRED (Advanced Lead Fast Reactor European Demonstrator) and to provide experimental data for code validation. HERO consists of a bundle of seven bayonet tubes characterized by an active length of six meters (1:1 with the ALFRED steam generator tube length). The main purposes of the research were to investigate the thermal hydraulic behavior of the innovative concept and provide a set of experimental data aiming at validating STH (System Thermal-Hydraulic) code. The calculations were carried out adopting RELAP5-3D©, updating the nodalization scheme validated with the experimental data of CIRCE-ICE campaign. The experiment consists of a transition from forced to natural circulation in a loss of flow accidental scenario; in order to identify the initial conditions of the experiment, several full power conditions were

simulated. Starting from the reference steady state conditions, five transient tests were simulated to evaluate the effect of the reduction of the secondary mass flow rate (reduced from the nominal value to simulate the activation of the DHR system) and the effect of the heat losses compensation. According with the calculation, HERO test section offers excellent thermal-hydraulic behavior ensuring a sufficient natural circulation conditions to remove the decay heat in the short term.

Keywords

Pool thermal-hydraulics; Thermal stratification; Safety analysis; RELAP5-3D©; CIRCE; HERO

1- Introduction

The construction of a demonstrator reactor is a fundamental step for the LFR (Lead fast reactor) development. At this purpose, in the frame of LEADER project (Lead-cooled European Advanced DEmonstration Reactor), ALFRED (Advanced Lead Fast Reactor European Demonstrator) was presented as the scaled-demonstrator reactor for the LFR technology (Frogheri et al., 2013). The growing interest in the lead fast reactors, required to identify sources of financing. In this framework, FALCON (Fostering ALfred CONsortium) Consortium Agreement was signed on December 2013 and it was the first step for the construction of ALFRED. The purpose of FALCON is to obtain resources, at first, to complete the technology development and design face and then, to support the reactor construction phase (Frignani et al., 2017).

The configuration of the steam generator bayonet tubes (SGBTs) for ALFRED is an innovative concept based on super-heated steam double wall bayonet tube steam generator which allows the increase of the safety margin of the nuclear power plant, strongly reducing the probability of the interaction between primary and secondary coolant and detecting any leakages from the liquid metal or the steam, by monitoring the pressure of the helium inside the gap volume.

Sapienza University of Rome supports the Experimental Engineering Division by the ENEA Brasimone Research Center in the heavy liquid metal (HLM) technology development, in particular in the framework of STH code validation and safety analysis. In this frame, the CIRCE (CIRColazione Eutettico) pool facility has been refurbished to host the new test section, called HERO (Heavy liquid mEtal pRessurized water cOoled tubes), aimed to investigate a bundle of seven bayonet tubes characterized by the active length of 6 m, in scale 1:1 with the tubes which will compose the ALFRED SGBT concept.

The pre-tests analysis aims to investigate the transition between forced and natural circulation in a loss of primary flow scenario and to select the initial and boundary conditions for the SESAME validation benchmark (Tarantino et al., 2016).

In this paper, the main results of the pre-test calculations, carried out using the system code RELAP5-3D©, are exposed and discussed.

2- The experimental facility

CIRCE is a multipurpose pool type facility aimed to study innovative HLM systems; it consists of the main vessel, filled with about 70 tons of lead-bismuth eutectic (LBE) and designed to host different test sections welded to the bolted heads, and two auxiliary tanks, intended to store the liquid metal during the upkeep phases and to maintain the LBE during the transfer phases (Narcisi et al., 2017a) (Turroni et al., 2001).

The test section, hung from the head of the main vessel, is the same used during the ICE (Integral Circulation Experiment) experimental campaign (Martelli et al., 2016) except for the heat exchanger (HX) which is substituted with the new steam generator. The test facility aims to reproduce the primary system of an innovative LFR, highlighting the thermal-hydraulic behavior of the steam generator bayonet tube (Frogheri et al., 2013). Figure 1 shows a graphical rendering of the test facility and it highlights the positioning of HERO, which is inserted in a dedicated flange of the vessel heads and partially located inside the cylindrical shroud of the previous HX. The liquid metal flow path in the test section is

described with arrows in Figure 2; after descending the downcomer of the facility, the LBE enters the test section passing through the feeding conduit, which represents the inlet section of the primary system. The feeding conduit is equipped with a Venturi-nozzle flow meter, to measure the LBE mass flow rate passing through the fuel pin simulator (FPS), which consists of a bundle of 37 electrically heated pins; the main features of the heat source (HS) are summarized in Table 1. The relative position between the pins and the wrapper is fixed by three spacer grids which identify three zones in the FPS (see Figure 3): the bottom mixing zone, located upstream of the lower spacer grid, the active length between the lower and the upper spacer grid, and the top mixing zone downstream of the upper spacer grid. Moreover, the pins are kept in the correct positions with a lower grid, which guarantees the LBE inlet, and an upper grid, operating as the FPS cap, equipped with penetrations for the pins. The hot LBE exits the HS and it flows inside the fitting volume, that connects the FPS with the riser, a double wall pipe insulated with an air gap in order to reduce the heat dissipation towards the pool. At the inlet section of the riser, the nozzle of the argon injection system is installed in order to inject the gas and to enhance the circulation of the primary coolant. The mixture flows upward and enters the separator, which is the upper component of the unit. The separator has two functions: it creates the expansion volume dedicated to the separation of the argon gas from the hot LBE and it guarantees the connection between the riser and the SG. The HERO SGBTs consists of seven double wall bayonet tubes with an active length of 6 m, arranged in a hexagonal bundle (Rozzia et al., 2017). The unit is included inside a double wall wrapper that consists of an internal hexagonal wrap and an external cylindrical shroud; the annular volume is filled by air to thermally insulate the unit. The hot LBE enters the unit through six inlet holes, obtained on the hexagonal shroud and located inside the separator, and it flows downward across the free volume between the inner wrap and the tubes. Figure 4 shows a schematic view of the bayonet tube: the feed-water enters at the top edge of the slave tube and flows downward, becoming saturated, it

is collected in the lower plenum of the tube and flows upward through the annular volume between the inner and the outer tube, where it reaches the superheated steam condition at the end of the active length. Afterward, the steam exits the unit and it is collected inside the steam chamber, hydraulically connected with each tube. The volume between the slave tube and the inner tube is filled with an insulating layer to prevent the steam condensation on the outer wall of the inner tube. The main features of the unit are the double separation and the leakage monitoring system. The separation between primary and secondary coolant is obtained with the second and the third tube; the volume between these two tubes is filled with pressurized helium, in order to detect any leakages from primary or secondary side by monitoring the gas pressure, and a high conductivity powder to enhance the heat exchange capability. The bayonet tubes are arranged inside the hexagonal shroud with a p/d of 1.42 and they are kept in position by means of five spacer grids (Narcisi et al., 2017a). In the experimental campaign, that will be performed on the test facility, the HERO heat exchanger will operate as SG during the full power conditions while, in accident transients, it operates as decay heat removal system (DHR), with a reduced feed-water mass flow rate, simulating the presence of an Isolation Condenser.

Table 1. FPS main parameters

Parameter	Value
Active length	1000 mm
Pin Diameter	8.2 mm
Pitch to diameter ratio	1.8
Nominal thermal power	800 kW
Thermal power per pin	25 kW
Heat flux at the pin wall	1 MW/m^2

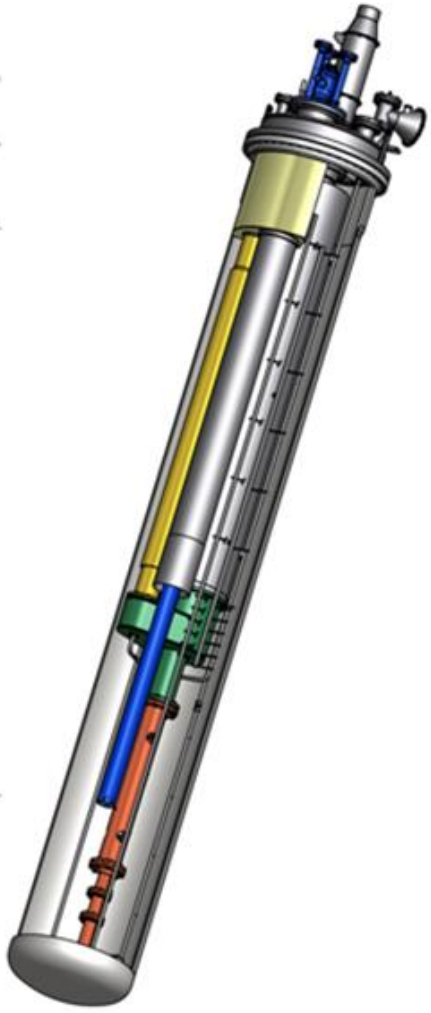

Fig. 1. CIRCE-HERO test facility

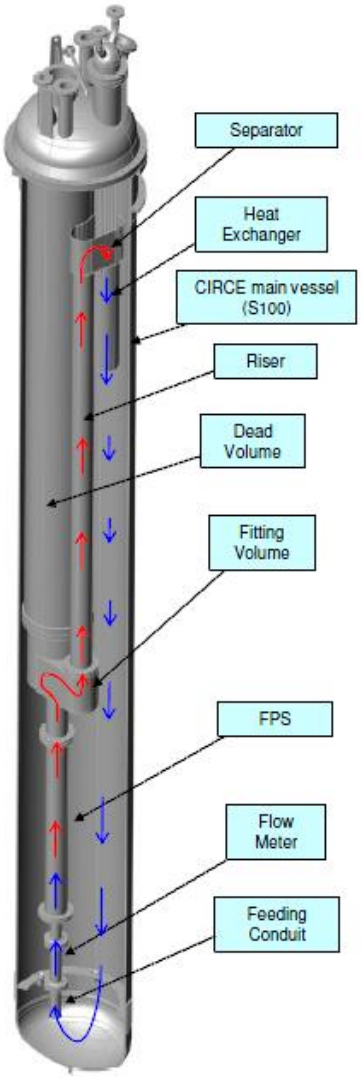

Fig. 2. Primary main flow path

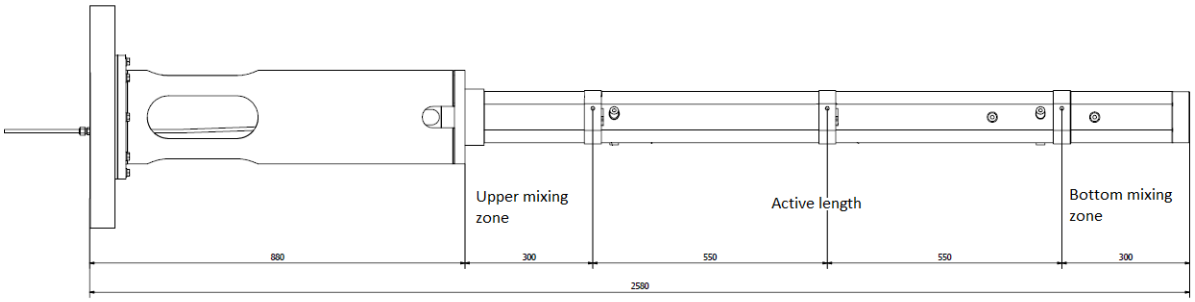

Fig. 3. FPS arrangement

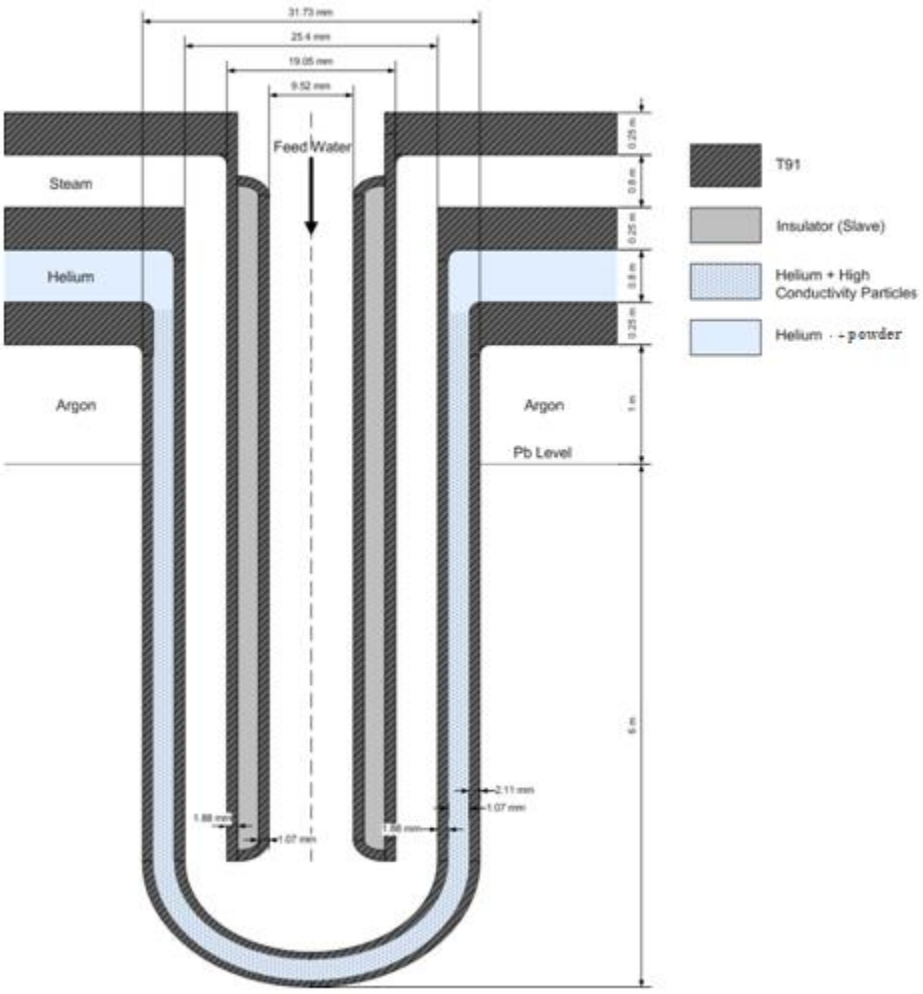

Fig. 4. HERO steam generator bayonet tube

3- RELAP5-3D© modeling

The RELAP5 series has been developed at Idaho National Laboratory (INL). The main application of the code is the simulation of transients in light water reactors (LWR) but it can be used to simulate various thermal-hydraulic transients in a wide range of both nuclear and non-nuclear systems. RELAP5-3D© (R5-3D) is the latest in the RELAP5 series; the main features which characterize R5-3D are the fully integrated, multi-dimensional (MULTID) thermal-hydraulic and kinetic modeling capability. The MULTID component has been introduced to better reproduce the three-dimensional phenomena that can be exhibited in any component of a LWR, such as the downcomer, the lower plenum or the core. Another

enhancement included in R5-3D is the addition of new working fluids, including HLMs for the Gen IV reactors simulation (The RELAP5-3D© Code Development Team, 2015b).

The nodalization scheme of CIRCE-ICE test facility, validated by the comparison with experimental data (Narcisi et al., 2017), has been upgraded to introduce the new test section: the HERO SGBTs substitutes the previous HX, the holes on the cylindrical shell of the FPS are closed (to limit the heat losses between the HS and the cold pool), and the DHR system is removed.

The nodalization scheme consists of two macro-regions, coupled to simulate the global facility: a mono-dimensional model, to reproduce the thermal-hydraulics of the primary main flow path (see Figure 5), and a three-dimensional component, shown in Figure 6, where the internals are depicted only to display the positioning, to investigate the thermal stratification and mixing convection phenomena and to identify the new thermocouples layout into CIRCE main pool.

The mono-dimensional model includes: the feeding conduit, the fuel pin simulator, the release pipe, the fitting volume, the riser, the separator and HERO (primary and secondary side). The FPS is analyzed sub-channel by sub-channel modeling the HS with 72 parallel pipes, each one divided into 15 control volumes. The pipes are linked with 1536 cross junctions in order to reproduce the mass transfers between adjacent sub-channels and to arrange every sub-channel in the right position, as shown in Figure 7. The thermal power supplied by the 37 pins is obtained with 5760 heat structure active nodes; other 1728 thermal nodes model the heat dispersion through the hexagonal wrapper and 3456 nodes, assuming a “fake” material with a negligible heat capacity and the LBE thermal conductivity, are added to simulate the thermal conduction into the fluid. The nodalization scheme of the FPS is created to compare the LBE temperatures in the exact position of the thermocouples (TCs) installed inside the HS. For the evaluation of the heat transfer coefficient (HTC) in a rod

bundle geometry for liquid metals, the Todreas & Kazimi correlation, implemented in R5-3D (The RELAP5-3D© Code Development Team, 2015a), is employed:

$$Nu = 4.0 + 0.33\left(\frac{p}{d}\right)^{3.8}\left(\frac{Pe}{100}\right)^{0.86} + 0.16\left(\frac{p}{d}\right)^{5}$$

where Pe is the Peclet number. This correlation was developed in the pitch to diameter ratio (p/d) range 1.1<p/d<1.4 and 10<Pe<5000. Previous activities on HLM technologies highlighted that an underestimation of the HTC occurs using this correlation, especially for a pitch to diameter ratio higher than 1.2 (Giannetti et al., 2016). A better estimation of the coefficient can be obtained using the Ushakov correlation (Ushakov et al., 1977), not implemented in the current version of R5-3D:

$$Nu = 7.55\frac{p}{d} - 20\left(\frac{p}{d}\right)^{-13} + \frac{3.67}{\left(90\frac{p}{d}\right)^{2}}Pe^{\left(0.56+0.19\frac{p}{d}\right)}$$

Considering that, in the operational range of temperature, the two correlations have a similar gradient of Nu versus Pe, an artificial multiplication factor of 1.31 is evaluated as the ratio between Ushakov correlation (using a p/d equal to the real value of 1.8) and Todreas & Kazimi correlation (using the maximum accepted value of the p/d), in the range of the working temperatures and assuming the nominal flow conditions. For non-bundle geometry, the Seban-Shimazaki correlation is used (The RELAP5-3D© Code Development Team, 2015a):

$$Nu = 5.0 + 0.025Pe^{0.8}$$

The argon injection at the riser inlet section is simulated with boundary conditions: the time-dependent volume sets the gas inlet conditions and the time-dependent junction, connected with the bottom edge of the riser second control volume, adjusts the mass flow rate injection. The pressure of the gas plenum of the facility is regulated by an additional time-dependent volume, that simulates the gas extraction through the gas circuit.

The SG primary side is simulated with a single equivalent pipe composed of 43 control volumes and hydraulically coupled at the top edge with the separator and at the bottom edge with the 3D component. The secondary side of the SGBTs is collapsed in two equivalent pipes: the first one for the descending side and the second one for the annular riser. The feed-water inlet conditions are set with the time-dependent volume, connected with the inlet section of the descending pipe with the time-dependent junction that sets the inlet mass flow rate. Another time-dependent volume is connected with the upper zone of the ascending pipe to fix the pressure at the steam chamber exit. The components that simulate the HERO SGBTs are thermally coupled with 4 heat structures; in particular, the heat structure which couples the LBE and the steam side, is adjusted with a calibrated multiplication factor, calculated as the ratio between Ushakov correlation (p/d = 1.42) and Todreas & Kazimi correlation (p/d = 1.4), to better reproduce the HTC.

The pressure drop across the Venturi nozzle and the grids, installed inside the FPS and the steam generator, are reproduced with a concentrated pressure loss coefficient K, dependent on the flow conditions and validated with post-test analysis conducted on the CIRCE-ICE campaign (Narcisi et al., 2017b) (Narcisi et al., 2017).

The mono-dimensional scheme is hydraulically coupled with the MULTID component by three junctions. Both the models are consistent with the vertical sliced approach. The MULTID component is composed of 51 axial levels, 4 radial meshes and 8 azimuthal. The number of azimuthal and radial meshes is chosen on the basis of the geometrical position of the internal components and porosity factors are used to reproduce the volume occupied by the internals.

The dimensions of the global model are summarized in table 2.

Table 2. Model dimensions

Parameter	Value
Number of hydrodynamic volumes	2942
Number of hydrodynamic junctions	7565
Number of heat structure mesh points	21153

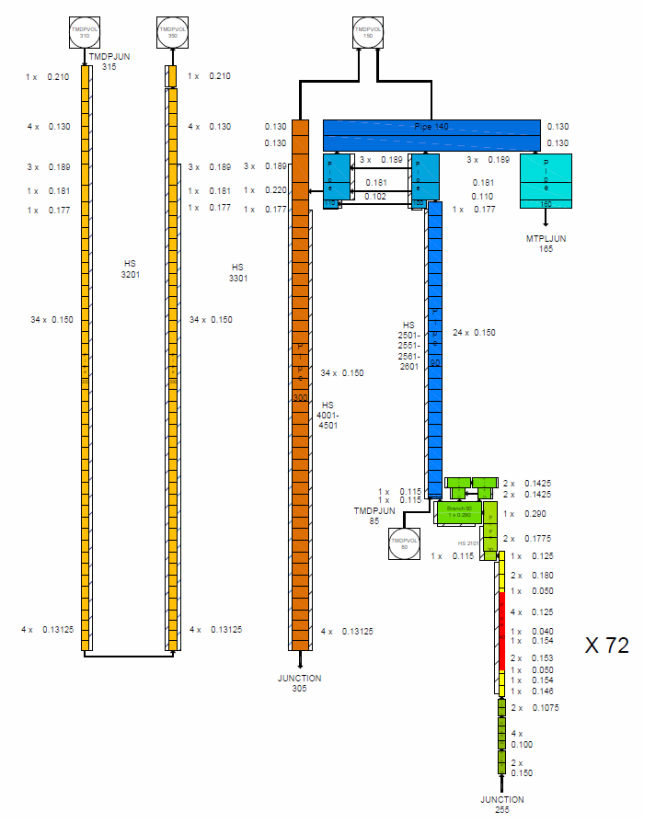

Fig. 5. Nodalization scheme: 1-D model

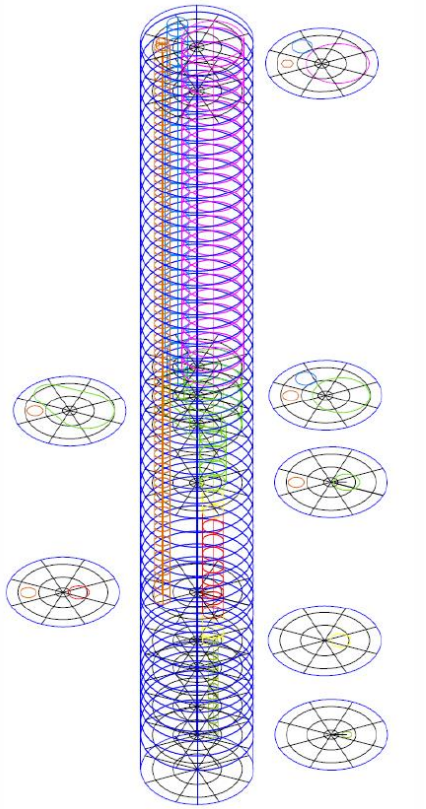

Fig. 6. Nodalization scheme: 3-D component

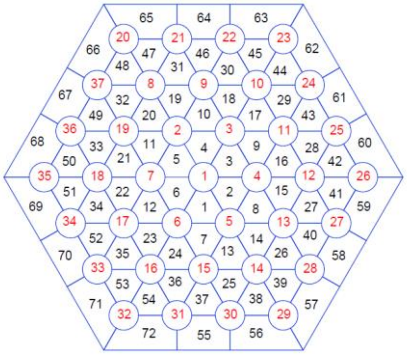

Fig. 7. Nodalization scheme: FPS model

4- Pre-Test Calculations

The main purposes of the pre-test analysis are to test the configuration of the SGBT candidate for ALFRED and to investigate phenomena such as the thermal stratification and the mixing convection inside a HLM pool.

4.1- Identification of full power steady-state conditions

The experiment consists in the transition from forced to natural circulation occurring in a loss of flow accidental scenario. Every simulation is carried out using the most accurate correlations for the LBE thermo-physical properties, recommended by NEA (OECD/NEA Nuclear Science Committee, 2015) and implemented in RELAP5-3D© (Balestra et al., 2016). To identify the initial conditions of the transient tests, several full power conditions are analyzed. The initial and boundary conditions of each case are summarized in Table 3. The case 1 is carried out to achieve a constant temperature drop across the FPS equal to 80 K in the range 673-753 K, which is representative of the temperature drop across the ALFRED core. The second one aims to obtain the LBE mass flow rate across the SG equal to 44.7 kg/s, representative of the scaled down SG of ALFRED. From case 1 to 6 the boundary conditions are the same, except for the Ar mass flow rate injected inside the test section, as shown in Table 3.

Table 3. Full power calculations: boundary conditions

Parameter	**Case 1**	**Case 2**	**Case 3**	**Case 4**	**Case 5**	**Case 6**
FPS thermal power (kW)	450.0					
LBE avg. pool T (K)	669.0					
Ar flow rate (Nl/s)	1.290	2.354	2.242	2.130	1.850	1.790
Steam pressure (bar)	172.0					
Feed-water (FW) inlet T (K)	608.0					
FW mass flow rate (kg/s)	0.331					

The main results, after 30000 s of simulation time, are summarized in Table 4. The full power steady-state, selected as the initial conditions for the transient simulations, is the case 1. Figure 8 shows a zoom of the boundary conditions in the first 3000 seconds, which remain constant up to the end of the calculation. The simulation begins in steady-state conditions with the HS turned off and the injection of the argon and the feed-water disabled. At 50 s, the injection of the Ar starts and the LBE mass flow rate reaches the value of 36.5 kg/s, as shown in Figure 9. After 220 s from the beginning of the calculation, the HS starts to supply the thermal power up to the nominal value at 390 s and the mass flow of the primary coolant increases to the value of 38 kg/s. The temperature of the whole system increases (see Figure 10) and at 2000 seconds the feed-water system is activated and the primary mass flow rate reaches the nominal value of 39.2 kg/s. After the activation of the FPS, the LBE temperature at the outlet section of the heat source increases: the heat dissipations through the hexagonal shroud of the fuel pin simulator cause a temperature drop between the internal and the external subchannels (respectively IC and EC in Figure 10) of about 25 K, as shown in Figure 11, where the LBE temperature at the end of the calculation is depicted sub-channel per sub-channel for five sections of the heat source. The temperature is uniform at the inlet of the heating unit and the effect of the heat dissipation increases along the FPS. Up to 2000 seconds, there is not a temperature drop through the primary side of the SG and the temperature of the primary coolant follows the same trend of the outlet of the FPS. When the feed-water is injected, after a delay time of about 450 s, the temperature at the outlet section of the heat source and at the SG inlet section reaches the maximum value. The steam generator starts to remove thermal power and the LBE SG outlet temperature rapidly decreases to the value of 690 K. After reaching the nominal boundary conditions, the temperature of the main flow path decreases to the nominal value (summarized in table 4). Figure 12 is a representation of the LBE temperature at the end of the simulation in the most representative section of the pool, which includes the FPS and HERO SG. The figure

highlights the temperature difference between the internal components and the LBE inside the pool, where the temperature quickly becomes uniform at the same vertical level and a thermal stratification phenomenon occurs at about 2.8 m from the bottom of the vessel. The level of the thermal stratification is influenced by the heat dissipation from the internal components, occurring at the same level of the hottest zone of the HS.

The LBE free level, initially set to 7.986 m from the bottom of the vessel (0.33 m from the bottom wall of the separator), moves during the operation, due to the overall pressure drop and the thermal expansion of the LBE. The difference of the free level between the pool and the separator of about 200 mm (see Figure 20) provides an estimation of the overall irreversible pressure drop of the main flow path. According to the CIRCE-ICE experimental results, an important portion of the global pressure drop is due to the Venturi-nozzle flow meter (0.096 bar); the irreversible pressure drop which occurs through the primary side of the SG, is calculated as about two times the flow meter value (0.2 bar).

Table 4. Full power calculations: main results

Parameter	Case 1	Case 2	Case 3	Case 4	Case 5	Case 6
FPS LBE inlet T (K)	677.0	672.5	672.3	672.1	671.5	671.2
FPS LBE average outlet T (K)	760	740.9	741.4	742.0	743.8	744.3
HERO LBE inlet T (K)	753.8	732.3	733.2	733.6	734.7	734.9
HERO LBE outlet T (K)	677.1	672.5	672.2	672.2	671.5	671.1
LBE mass flow rate at inlet section of HERO (kg/s)	39.2	44.5	43.9	43.4	42.1	41.7
Power removed by HERO (kW)	438.0	440.0	439.0	439.0	438.0	440.0
Steam max T (K)	672.1	659.2	659.1	659.1	659.1	658.8
Heat losses (kW)	12.0	10.0	11.0	11.0	12.0	10.0

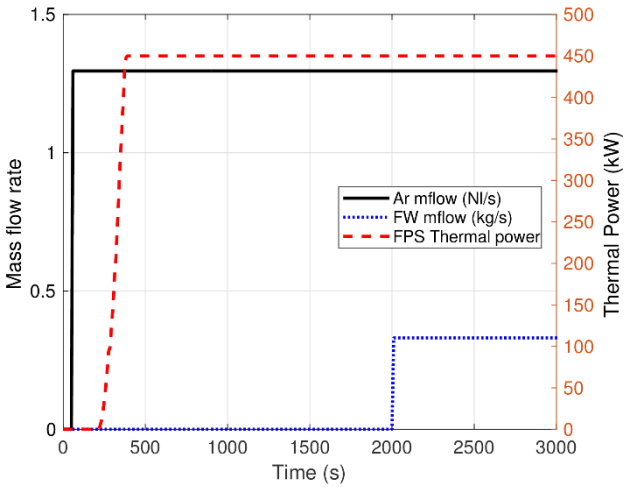

Fig. 8. Full power calculation: boundary conditions

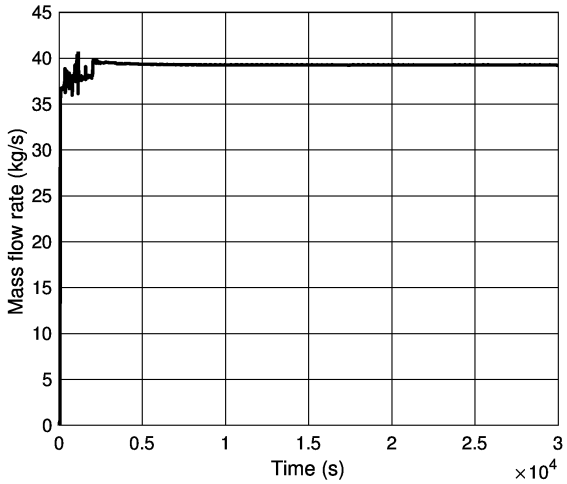

Fig. 9. Case 1: LBE mass flow rate

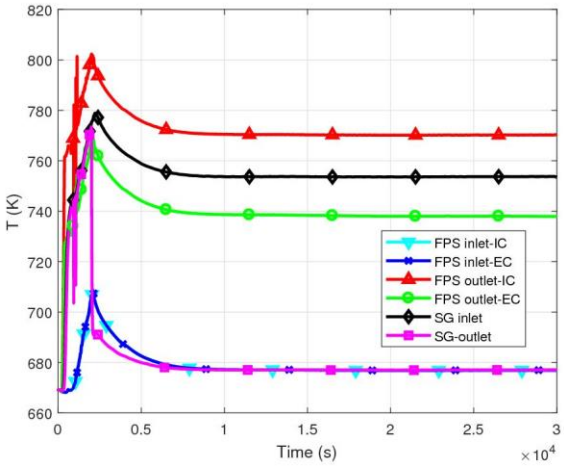

Fig. 10. Case 1: LBE temperatures

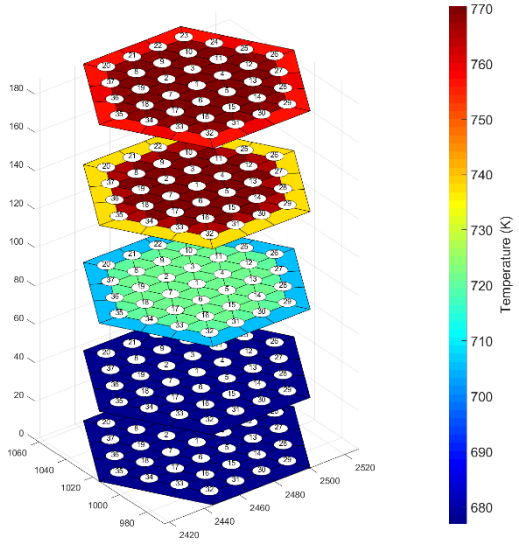

Fig. 11. Case 1: FPS temperatures

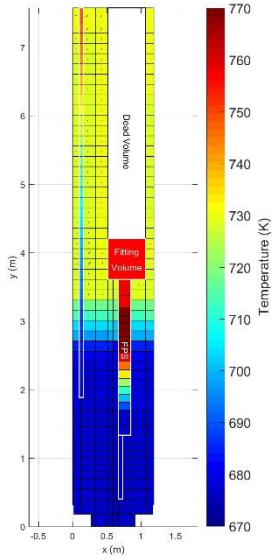

Fig. 12. Case 1: pool temperatures

4.2 -Transient analysis

The starting point for the transient analysis is the full power steady-state conditions of the case 1. In order to select the reference accidental scenario, five transient tests are evaluated. The first one (TrT 1) consists of a protected loss of primary pump in which:

- the argon injection decreases to 0 following a calibrated curve simulating the presence of a pump flywheel;

- the thermal power supplied by the HS reproduces a decay heat curve, scaled down from a reference curve for fast reactor and compensated with the heat losses through the main vessel;
- the feedwater mass flow rate decreases to 10% of the nominal value to simulate the activation of the DHR system.

The second calculation (TrT 2) aims to investigate the effect of a higher value of the feed-water flow rate injected inside the test section; the boundary conditions are the same of the transient test 1, except the feed-water mass flow rate, set to 20% of the nominal value. The transient test number three (TrT 3) consists of a loss of primary pump plus a loss of DHR function in hot condition, maintaining the same boundary conditions of TrT 1, except for the feed-water injection which decreases to zero. The transients 4 and 5 aim to investigate the effect of the compensation of the heat losses; they maintain the same boundary conditions of the TrT 1 and 3, respectively, except for the decay curve which is not compensated with the value of the heat losses.

The simulation time of each transient simulation is 1000 seconds and the boundary conditions are depicted in Figure 13, where the attention is focused on the first 300 seconds. In each transient simulation, the feed-water mass flow rate instantly decreases to the final value; the thermal power of the HS rapidly decreases below 100 kW and at about 150 s reaches the compensated decay power. The argon injection system sustains the circulation of the LBE during the transient beginning; at about 25 seconds, when the thermal power is close to the compensated decay power, the argon mass flow rate is still 50% of the nominal value and only after 300 s it becomes zero. The comparison of the compensated and non-compensated decay curve is depicted in Figure 14.

The main events of the transient test 1 are summarized in Table 5. Figure 15 and 16 depict the evolution of the LBE mass flow rate at the inlet section of the SG and the inlet and outlet temperatures of the FPS and HERO. As result of the chain of events described in Figure 13,

the temperature at the outlet section of the HS rapidly decreases to the minimum value of 690 K. At this time, the LBE mass flow rate is close to 50% of the nominal value and the thermal power of the HS near to the compensated decay power; it causes the minimum value of the temperature drop across the FPS and, after a delay time of about 30 s, also the minimum value of the temperature drop across HERO test section, when the LBE exiting the SG reaches the maximum value of 715 K. As shown in Figure 16, the SG inlet temperature is not affected by the temperature trend at the outlet of the FPS. This is due to the thermal inertia of the large volume of liquid metal contained inside the separator and to the low value of the primary mass flow; therefore, the LBE temperature inside the separator decreases slower than in the components upstream.

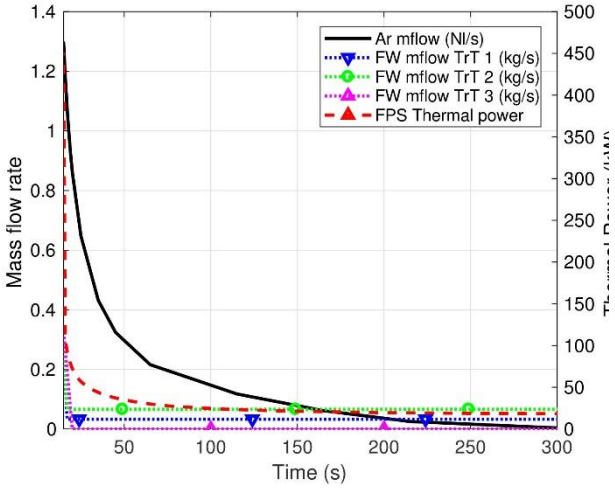

Fig. 13. Transient test: boundary conditions

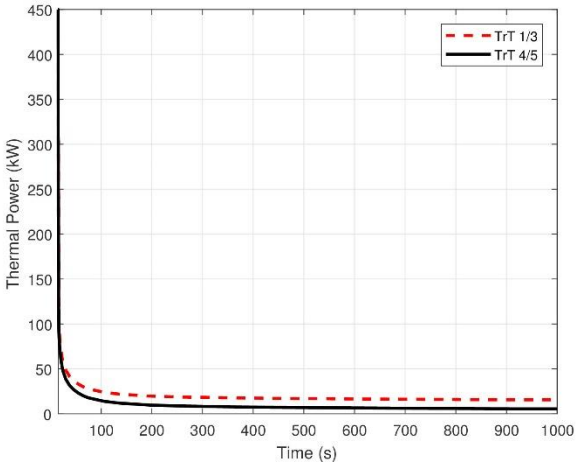

Fig. 14. Transient tests: decay heat curve

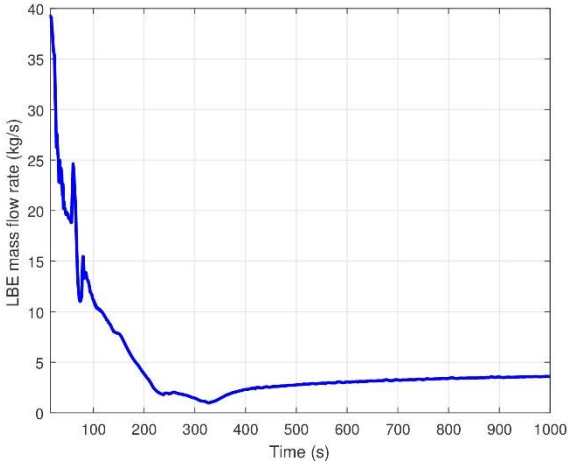

Fig. 15. TrT1: LBE mass flow rate

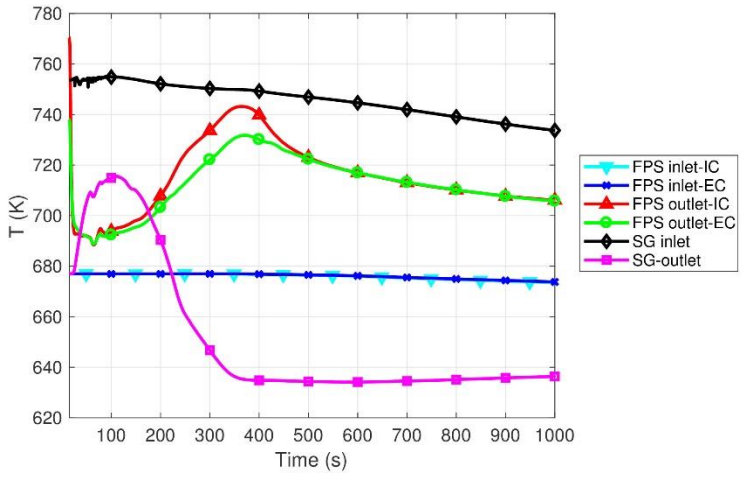

Fig. 16. TrT1: LBE temperatures

At about 25 seconds, the oscillation of the LBE mass flow rate is caused by the fluctuation of the free level that passes through two contiguous control volumes inside the separator. When the argon injection is disabled, the primary mass flow rate reaches the minimum value of 1.4 kg/s and the FPS outlet temperature amounts to the peak value of 745 K, remaining lower than the nominal value at the beginning of the test. At the same time, the temperature drop across the steam generator increases and the LBE outlet temperature reaches the minimum value of 630 K, lower than the LBE temperature inside the pool, as shown in Figure 17 c. The LBE mass flow rate increases to the value of 3.7 kg/s and the average temperature of the global system decreases. The Figure 17 shows the evolution of the temperature inside the main vessel during the transient test, highlighting that, at the thermal stratification level, the vertical gradient of the temperature is reduced respect to steady-state conditions, as shown also in Figure 18 where the LBE temperature inside the pool is plotted versus the elevation from the bottom of the vessel. This phenomenon is due to the hot LBE exiting the SG during the first moments of the transient test. After 350 s, the LBE exiting the HERO subchannels is cooler than the liquid metal inside the pool, which starts to decrease its temperature and causes the vertical trend at the end of the test. The Figure 19 summarized

the evolution of the LBE temperature inside the FPS, depicted sub-channel per sub-channel, as previously described.

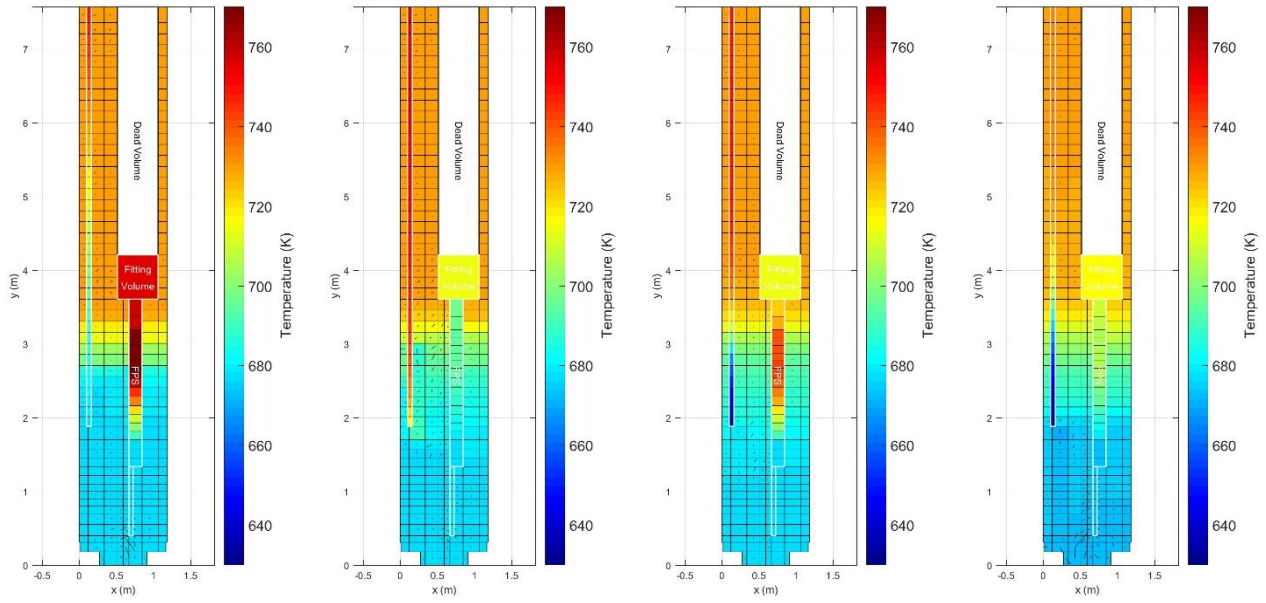

A B C D

Fig. 17. TrT 1: pool temperature evolution. a) 0 s; b) 110 s; c) 350 s; d) 1000 s

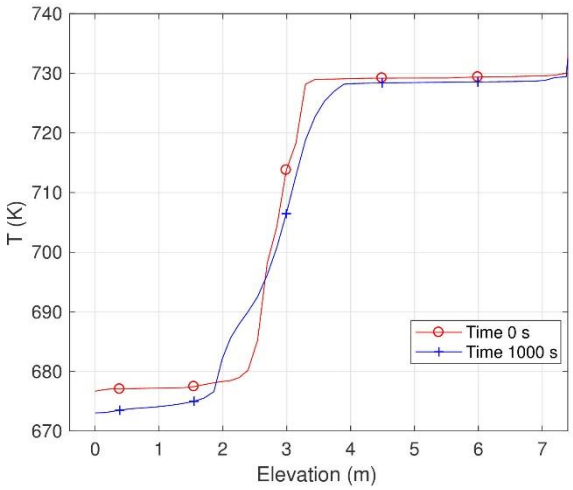

Fig. 18. TrT 1: thermal stratification

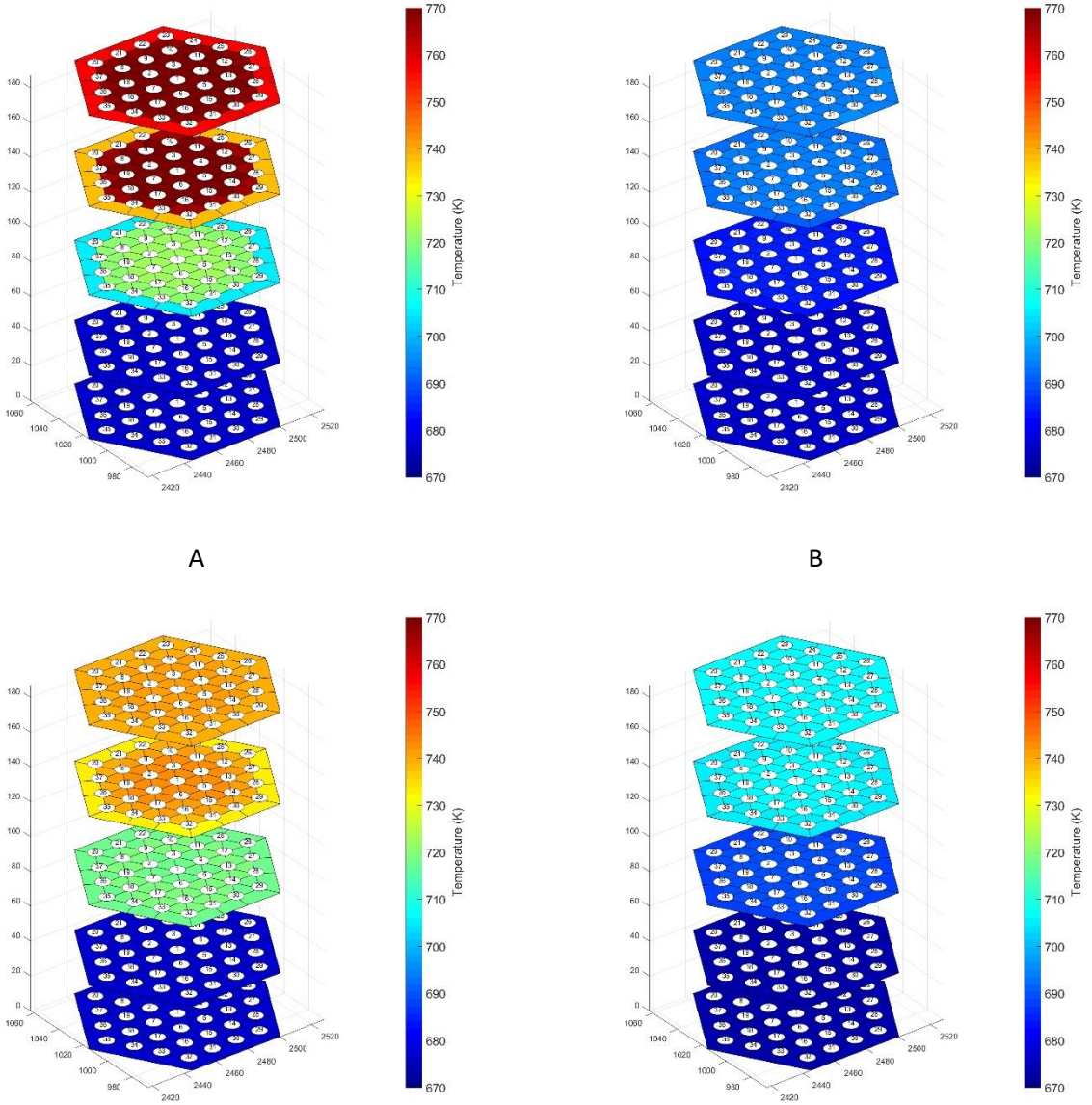

A B

C D

Fig. 19. TrT 1 – FPS temperature evolution. a)0 s; b)80 s; c)350 s; d)1000 s

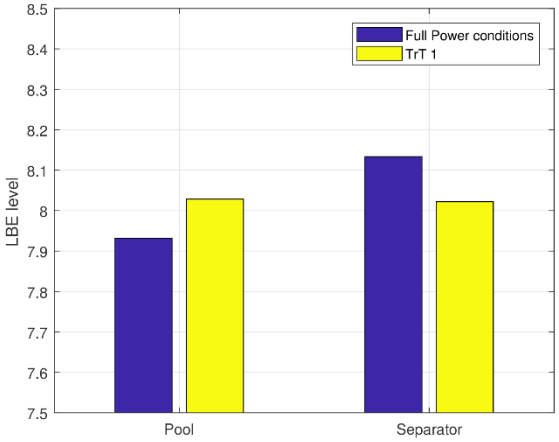

Fig. 20. LBE free levels

A lower value of the LBE mass flow rate causes a reduction of the irreversible pressure drops: across the Venturi-nozzle flow meter and the HERO test section the pressure drops are respectively decreased to the values of 74 and 355 Pa. As a consequence of the reduction of the pressure drop through the main LBE flow path, the level inside the separator and pool moves, respectively, downstream and upstream of about 100 mm, as shown in Figure 20, where the positions of the free level inside the separator and the pool are compared with the position at the beginning of the test.

Table 5. Transient test 1: main events

Time (s)	**Main event**
0	Start of the transient sequence
80	Minimum value of the LBE temperature at the outlet section of the FPS
110	Peak temperature at SG outlet section
340	Minimum value of the LBE mass flow rate
350	Peak temperature at the outlet section of the FPS and minimum temperature at the outlet of HERO
1000	End of the transient test

The following analysis concerns the comparison of the results of TrT1, 2 and 3. Figure 21 shows the LBE mass flow rate at the inlet section of HERO; during the first 50 seconds, the primary flow is still influenced by the argon injected into the riser (see Figure 13) and the trend of the three simulations is similar, as the LBE temperature at the inlet and outlet section of the FPS and SG (see Figure 22 and 23). After 150 s, the injection of the gas is decreased enough to highlight differences between the three calculations: the most important contribution to the driving force is the natural circulation, promoted by the thermal power removed by the SG, and the LBE mass flow in test 2 is constantly greater than in tests 1 and 3. In particular, during the transient 3, the driving force only depends on the heat losses

through the main vessel, since the feed-water injection is halted. In this case, the LBE temperature at the SG outlet reaches the maximum value of 738 K, at about 110 s, remaining higher than 730 K up to 200 s (see Figure 23); at the same time the outlet temperature of the FPS is close to the minimum value of about 690 K. Due to this thermal configuration, a natural circulation cell arises, opposing itself to the residual lift force exerted by the driving gas. This gas flow, in the absence of the feedwater contribution, it is no longer sufficient to push the LBE inside the FPS, causing the temperature peak of 738 K at the inlet of the HS (see Figure 22). The liquid metal reverse flow is maintained between 220 and 370 s, as it can be observed in Figure 21; afterward, the gradual heating of the FPS, due to the decay heat, weakens the temperature gradient responsible for the opposing circulation and the forward flow are restored, assuming the value of 0.5 kg/s. Due to the compensation of the heat losses, the temperature of the whole system increases reaching, at the outlet of the FPS, the maximum value of 820 K, close to the maximum temperature experimentally allowed.

In Figure 24, the LBE temperature inside the pool versus the elevation is plotted to compare the final conditions of each calculation. The expansion of the thermal stratification zone, highlighted at the end of the transient test 1, also occurs during the TrT 2 and 3. At the end of test 2, the vertical trend of the temperature is similar to the final conditions of the TrT 1, assuming lower temperature in the bottom volume of the pool. Due to the higher temperature at the outlet section of the SG, in the transient test 3 the stratification zone is wider than in TrT 1 and 2, arriving at 1 m from the bottom of the pool. The LBE temperature is plotted in Figure 25 to highlight the thermal stratification position.

To evaluate the effect of the heat losses compensation, the transient tests 1 and 3 are repeated assuming the typical decay heat curve, as shown in Figure 14. Figure 26 shows the comparison between the TrT 1 and 4, plotting the LBE temperature at the inlet and outlet section of the HS and HERO. The main variation between the two calculations is the outlet

temperature of the FPS, where the difference of the thermal power supplied is highlighted by the LBE temperature which, in the case 4, is constantly lower than the case 1. Because of the duration of 1000 seconds and the low primary mass flow rate, no difference for the temperature field is found between the two simulations at the inlet section of the SG; this value only depends on the heat dissipation along the flow path which is comparable in both the calculations. The difference at the HERO outlet section is due to the slightly lower LBE mass flow rate during test 4 which causes a higher temperature drop across the steam generator. It is not enough to variate the LBE temperature inside the pool though, since the large heat capacity of the liquid metal absorbs the slight difference of temperature, causing the same temperature at the inlet of the FPS as shown in Figure 28.

The same parameters are plotted in Figure 27, comparing the results of the TrT 3 and 5. The main variation is still found for the outlet temperature of the HS (about 60 K at the end of the calculation). Notwithstanding the average outlet temperature increases during the test 5, at the end of the simulation the maximum temperature inside the HS is lower than the initial value. Another effect of the lower thermal power supplied is the decrease of the driving force that causes a primary mass flow near to zero; this is the reason of the large difference of the SG outlet temperature between the two calculations. After the restoration of the forward flow, in test 3, the LBE mass flow rate is enough to move the hot liquid to the bottom edge of the SG, reducing the temperature drop across the component. Instead, in test 5, the reverse flow decreases the outlet temperature to the value of 685 K, which remains practically constant up to 1000 s, due to the quasi-stagnant conditions that occur after the dissipation of the reverse flow. This effect is also highlighted by the FPS inlet temperature, where the very low value of the LBE mass flow is not enough to decrease too much the temperature from the peak of 710 K.

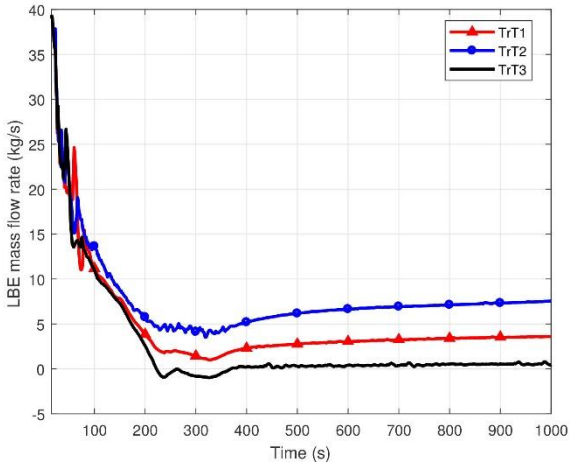

Fig. 21. First comparison: LBE mass flow rate

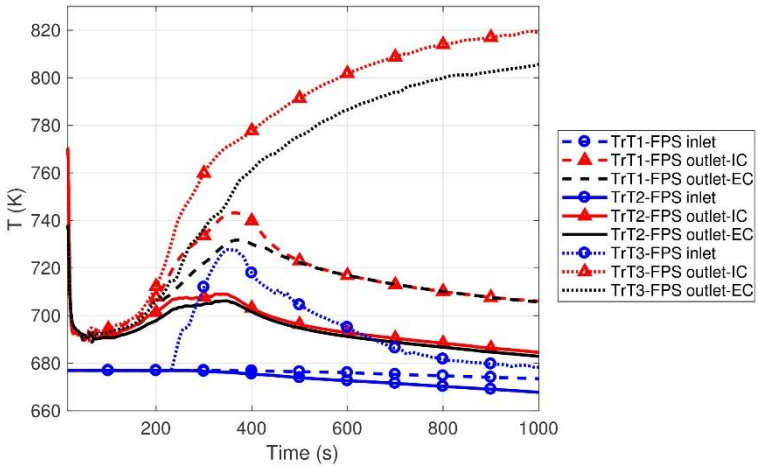

Fig. 22. First comparison: FPS temperatures

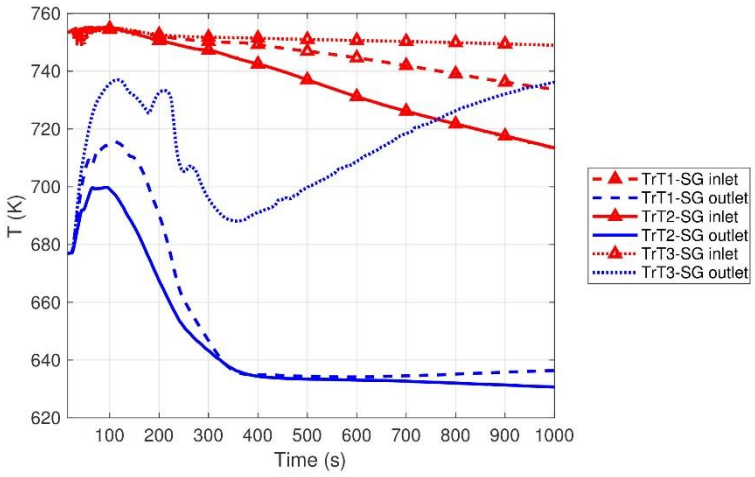

Fig. 23. First comparison: SG temperatures

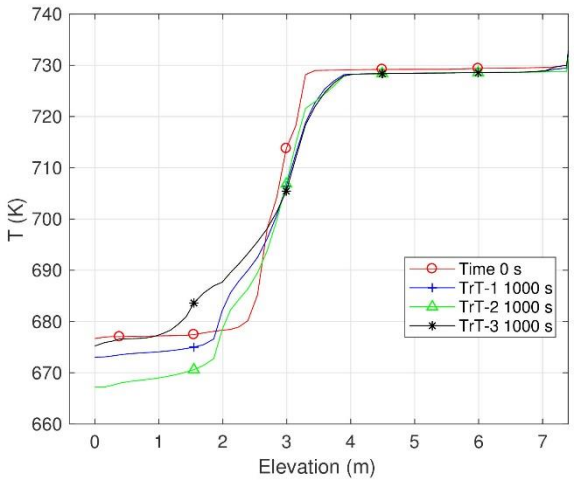

Fig. 24. First comparison: thermal stratification

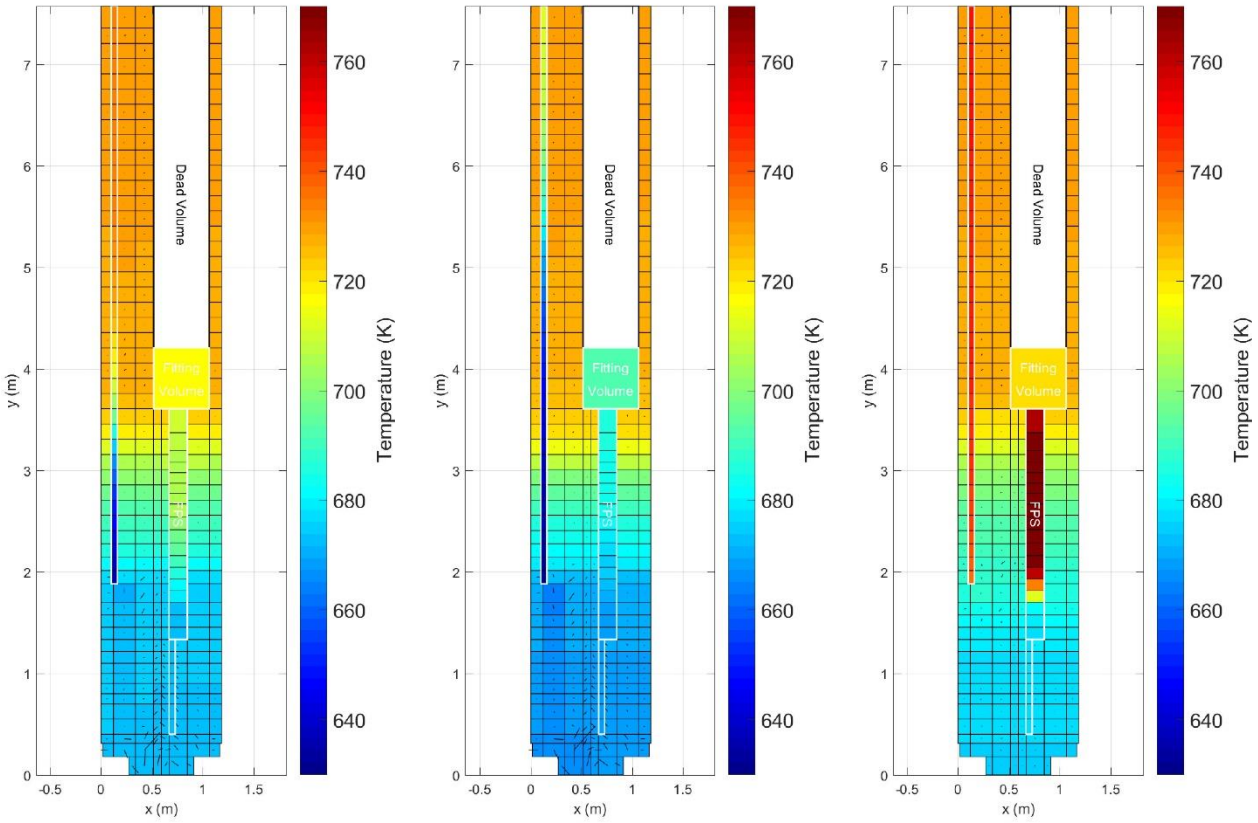

A B C

Fig. 25. First comparison: pool temperature. a) Transient test 1; b) Transient test 2; c) Transient test 3

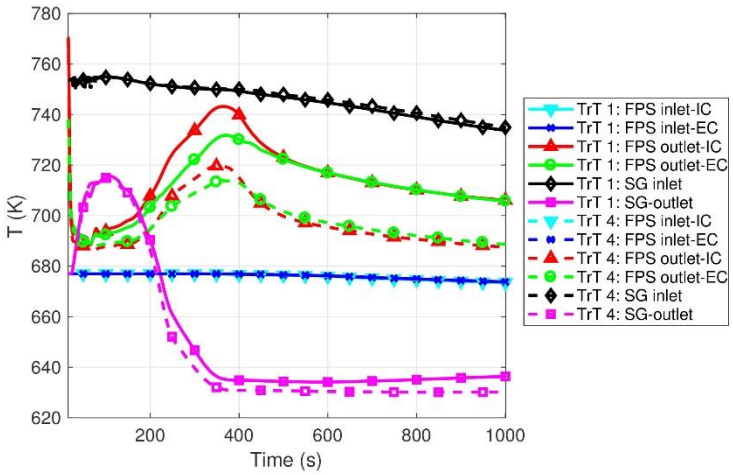

Fig. 26. Second comparison: LBE temperatures

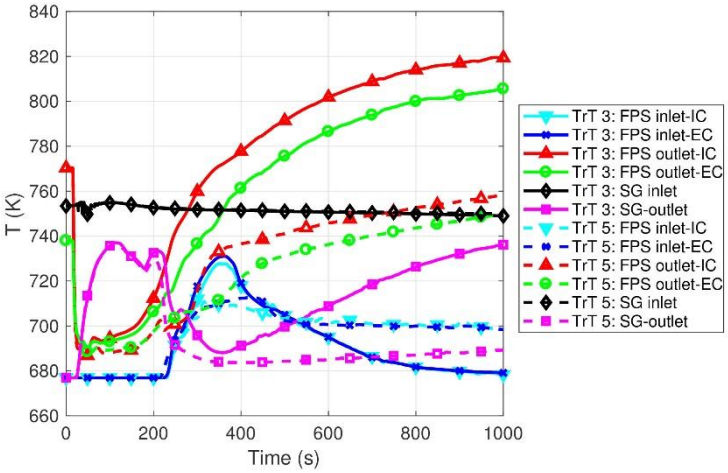

Fig. 27. Third comparison: LBE temperatures

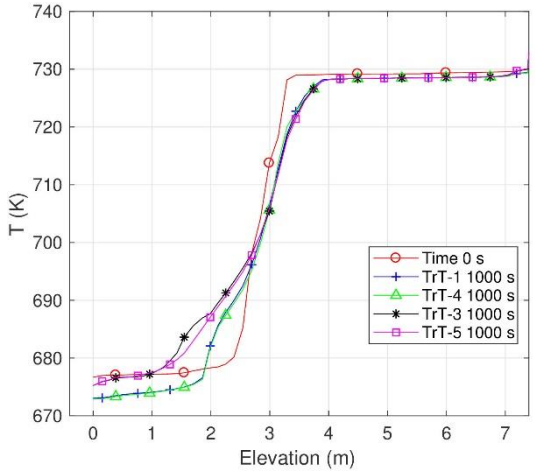

Fig. 28. Second and third comparison: Thermal stratification

5 Conclusions

The objective of this activity has been to carry out the pre-test analyses on CIRCE-HERO test facility, to evaluate the performance of the candidate steam generator bayonet tube for ALFRED reactor and to provide a set of reliable experimental data suitable for STH code validation. The simulations have been performed with RELAP5-3D© code, upgrading the validated model of CIRCE-ICE facility; the calculation has been carried out using the most recent correlation for the LBE thermo-physical properties, recommended by NEA and implemented in R5-3D. The analysis aimed to investigate the transition from forced to natural circulation in the loss of flow accident scenario. At first, a sensitivity analysis has been performed to identify the steady-state conditions that represent the initial conditions for the transient tests. After that, five transient calculations have been carried out: the transient tests 1 and 2 have simulated a protected loss of flow accident in which the HERO test section has simulated the activation of the DHR system, reducing respectively the feed-water mass flow rate to 10% and 20% of the nominal value. The transient test 3 has been identified to simulate the loss of primary pump plus the loss of DHR function in hot condition, reducing to zero the secondary mass flow rate. The three calculations are performed compensating the decay power with the heat losses through the main vessel. In order to evaluate the effect of this assumption, the transient test 1 and 3 have been repeated using a non-compensated decay heat curve. The simulation results have highlighted that the HERO test section guarantees a sufficient natural circulation conditions to remove the decay heat in the short term.

When the feedwater mass flow rate is deactivated, the code predicts the reverse flow of the primary coolant: this phenomenon will be experimentally investigated.

The calculations have provided useful information for the realization of the validation benchmark and the transient test 1 has been chosen as the reference scenario.

Acknowledgements

The SESAME project has received funding from the Euratom research and training programme 2014-2018 under grant agreement No 654935.

References

Balestra, P., Giannetti, F., Caruso, G., Alfonsi, A., 2016. New RELAP5-3D lead and LBE thermophysical properties implementation for safety analysis of Gen IV reactors. Sci. Technol. Nucl. Install. 2016. https://doi.org/10.1155/2016/1687946

Frignani, M., Grasso, G., Tarantino, M., Constantin, M., Turcu, I., Di Gabriele, F., Romanello, V., Alemberti, A., 2017. FALCON advancements towards the implementation of the ALFRED Project. Proc. Int. Con. Fast Reac. Rel. Fuel Cycl.: Next Gen. Nucl. Syst. Sust. Dev., Yekaterinburg, Russian Federation.

Frogheri, M., Alemberti, A., Mansani, L., 2013. The Advanced Lead Fast Reactor European Demonstrator (ALFRED). Proc. 15th Int. Top. Meet. Nucl. React. Therm. - Hydraul. Int. Top. Meet. Nucl. React. Therm. - Hydraul. 12, Pisa, Italy, May 2013.

Giannetti, F., Vitale Di Maio, D., Naviglio, A., Caruso, G., 2016. Thermal-hydraulic analysis of an innovative decay heat removal system for lead-cooled fast reactors. Nucl. Eng. Des. 305, 168–178. https://doi.org/10.1016/j.nucengdes.2016.05.005

OECD/NEA Nuclear Science Committee, 2015. Handbook on Lead-bismuth Eutectic Alloy and Lead Properties, Materials Compatibility, Thermal- hydraulics and Technologies. <https://www.oecd-nea.org/science/pubs/2015/7268-leadbismuth-2015.pdf>.

Martelli, D., Tarantino, M., Piazza, I. Di, 2016. Experimental Activity for the Investigation of Mixing and Thermal Stratification Phenomena in the CIRCE Pool Facility. Proc. 24th Int. Con. Nucl.Eng. 1–8. Charlotte, North Carolina, USA. June 2016. ICONE24-60920.

Narcisi, V., Giannetti, F., Del Nevo, A., Tarantino, M., Caruso, G., 2017a. Pre-test analysis

of protected loss of primary pump transients in CIRCE-HERO facility. J. Phys. Conf. Ser. 923 (012005). https://doi.org/10.1088/1742-6596/923/1/012005

Narcisi, V., Giannetti, F., Lorusso, P., Tarantino, M., Del Nevo, A., Caruso, G. Thermal Stratification analysis in CIRCE-ICE pool facility with RELAP5-3D model, in: Proc. of GLANST 2017 Global Symposium on Lead and Lead Alloy Based Nuclear Energy Science. pp. 298–299.Seoul, Republic of Korea, September 2017.

Narcisi, V., Giannetti, F., Tarantino, M., Martelli, D., Caruso, G., 2017b. Pool temperature stratification analysis in CIRCE-ICE facility with RELAP5-3D©model and comparison with experimental tests. J. Phys. Conf. Ser. 923 (012006). https://doi.org/10.1088/1742-6596/923/1/012006

Rozzia, D., Pesetti, A., Del Nevo, A., Tarantino, M., Forgione, N., 2017. HERO Test Section for Experimental Investigation of Steam Generator Bayonet Tube of Alfred. Proc. 25th Int. Con. Nucl.Eng. 1–10. Shangai, China. July 2017. ICONE25-67422.

Tarantino, M., Rozzia, D., Del Nevo, A., Giannetti, F., 2016. CIRCLE-HERO test setup. SESAME - 654935 - D4.3.

The RELAP5-3D© Code Development Team, 2015a. RELAP5-3D © Code Manual Volume IV : Models and Correlations. INL/MIS-15-36723 Volume IV, Revision 4.3.

The RELAP5-3D© Code Development Team, 2015b. RELAP5-3D Code Manual Vol.1 Code Structure, System Models and Solution Methods INL/MIS-15-36723 Volume I, Revision 4.3.

Turroni, P., Cinotti, L., Corsini, G., Mansani, L., 2001. The CIRCE test Facility, in: ANS Winter Meeting AccApp. Reno, Nevada, USA.

Ushakov, P.A., Zhukov, A.V., Matyukhin, N.M., 1977. Heat transfer to liquid metals in regular arrays of fuel elements. High Temperature 15, 868-873 (translated from Teplofizika Vysokikh Temperatur 15 (1977), 1027–1033).